IEEE Access
Multidisciplinary ⋮ Rapid Review ⋮ Open Access Journal

Received December 12, 2019, accepted December 25, 2019, date of publication December 30, 2019,
date of current version January 8, 2020.

Digital Object Identifier 10.1109/ACCESS.2019.2962909

An Optimal Monitoring Model of Desertification in Naiman Banner Based on Feature Space Utilizing Landsat8 OLI Image

BING GUO[1,3,4,5] AND YE WEN[2]

[1]School of Civil Architectural Engineering, Shandong University of Technology, Zibo 255000, China
[2]College of Land and Environment, Shenyang Agricultural University, Shenyang 110866, China
[3]Key Laboratory of Geomatics and Digital Technology of Shandong Province, Qingdao 266590, China
[4]Key Laboratory of Digital Earth Science, Institute of Remote Sensing and Digital Earth, Chinese Academy of Sciences, Beijing 100101, China
[5]State Key Laboratory of Information Engineering in Surveying, Mapping and Remote Sensing, Wuhan University, Wuhan 430079, China

Corresponding author: Ye Wen (yewen1990gbjl@163.com)

This work was supported in part by the Open Research Fund of Key Laboratory of Digital Earth Science, Chinese Academy of Sciences under Grant 2019LDE006, in part by the Project of Shandong Province Higher Educational Science and Technology Program under Grant J18KA181, in part by the Open Fund of Key Laboratory of Geomatics and Digital Technology of Shandong Province, in part by the National Key Research and Development Program of China under Grant 2017YFA0604804, and in part by the Open Fund of State Laboratory of Information Engineering in Surveying, Mapping and Remote Sensing, Wuhan University, under Grant 17I04.

ABSTRACT Current feature space models of desertification were almost linear, which ignored the complicated and non-linear relationships among variables for monitoring desertification. Fully considering the influencing factors of the desertification process in Naiman Banner, four sensitive indices including MSAVI, NDVI, TGSI, and Albedo have been selected to construct five feature spaces. Then, the precisions of different feature space models for monitoring desertification information (including non-linear and linear models) have been compared and analyzed. The non-linear Albedo-MSAVI feature space model for Naiman Banner has higher efficiency with the overall precision of 90.1%, while that of Albedo-TGSI had the worst precision with 0.69. Overall, the feature space model (non-linear) of Albedo-MSAVI has the highest applicability for monitoring the desertification information in Naiman Banner.

INDEX TERMS Albedo-MSAVI, monitoring model, feature space, Landsat8 OLI, Naiman Banner.

I. INTRODUCTION

Desertification, one of the most serious eco-environmental problems, has become a major land degradation type occurring over the world during the past decades [1]. Naiman Banner, located in Horqin Sandy Land (the typical region of semi-arid and semi-humid agro-pastoral ecotone in China), is experiencing extensive aeolian desertification accounting for 50% of the Naiman Banner [2]–[4]. Desertification has become a major environmental problem that is hampering socio-economic development and threatening its ecological environment in Naiman Banner under the joint actions of climate change and human activity [1].

Dynamic information of desertification is conductive to understand the desertification process and to establish early warning prevention projects for desertification [5]–[8]. However, field measurement is often limited due to the expensive cost, intensive labor, time-consuming and small spatial scale [9], [10]. Then, the remote sensing images have been utilized to interpret the extent of desertification, which is a subjective process [11], [12] evaluated the ecological vulnerability pattern in Naiman Banner under the influence of desertification, utilizing the comprehensive evaluation index method. Based on Landsat Images, [13] analyzed the relationships between levels of desertification and the surface water in Naiman Banner.In addition, automatic classification methods have often been utilized to obtain the desertification information in large area, however, the improvement of classification accuracy is limited to a certain extent. In recent years, the feature space model has been widely utilized to quantitatively obtain the desertification information, which could better reflect the land surface change information of desertification [8], [10], [14]. The feature space models have been constructed with some sensitive parameters

The associate editor coordinating the review of this manuscript and approving it for publication was Weipeng Jing.

for desertification, such as normalized difference vegetation index (NDVI), topsoil grain size index (TGSI), modified soil adjusted vegetation index (MSAVI), land surface albedo [15], [16]. However, the proposed monitoring models were almost linear, which ignored the complicated and non-linear relationships between different parameters of feature space.

In response to this challenge, the precisions of different feature space monitoring models for desertification (including non-linear and linear models) have been compared and analyzed, aiming to propose the optimal approaches for desertification in Naiman Banner. In this study, the NDVI, MSAVI, Albedo, and TGSI have been inversed utilizing Landsat 8 OLI image to construct different feature space models and then comparisons and analysis have been made to propose the optimal detection model of desertification.

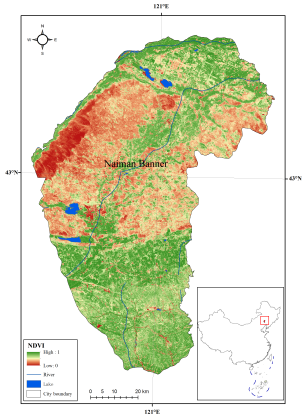

FIGURE 1. Location of the study region.

II. MATERIALS AND METHODS

A. DATA COLLECTION AND PREPROCESSING

The Landsat8 OLI image (available at https://glovis.usgs.gov/) was the main data source for establishing the detection model of desertification in Naiman Banner (Figure 1). The path/ row of image that utilized in this study are 121/30. In this study, the visible, near infrared and mid infrared wavelengths that composed of six bands with a spatial resolution of 30 m were utilized. Considering the influence of radiometric distortions and atmospheric perturbations on

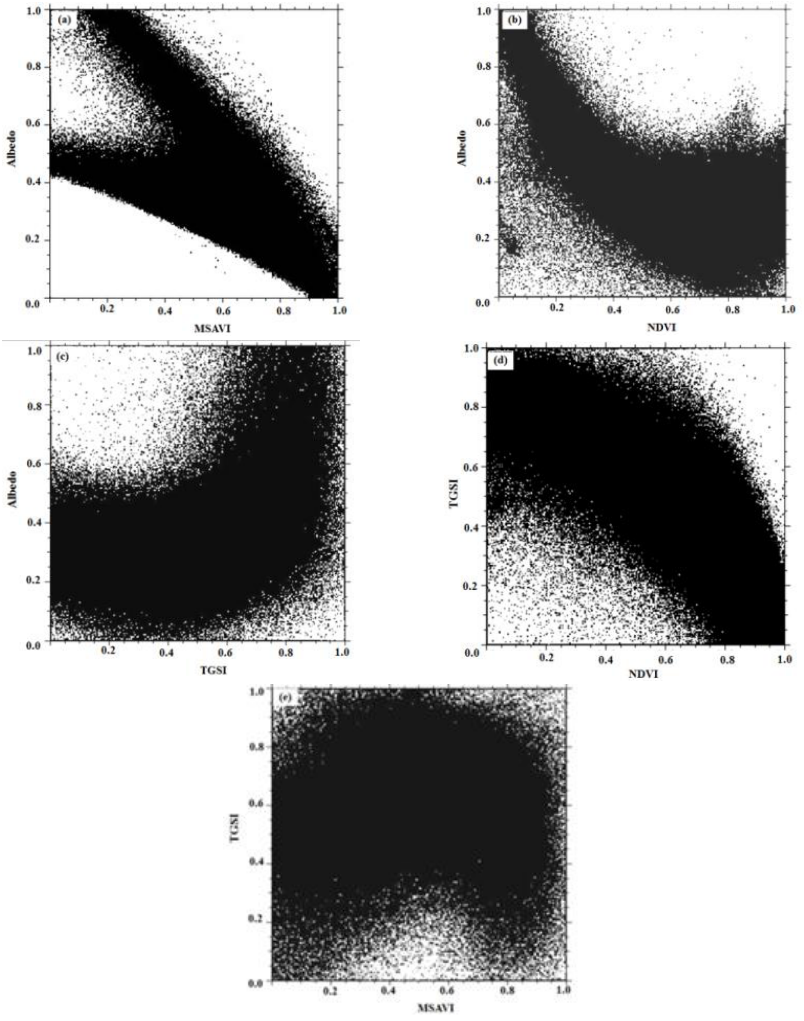

FIGURE 2. Five feature spaces for monitoring desertification (a) Albedo-MSAVI; (b) Albedo-NDVI; (c) Albedo-TGSI; (d) TGSI- NDVI; (e) TGSI-MSAVI.

the image quality, geometrical calibration and atmospheric correction had been conducted with ENVI 5.3. There were 210 verification points that obtained from Google Earth and field observation, which were set as 30 × 30 quadrats.

B. SENSITIVE INDICES FOR FEATURE SPACE

The radiant energy absorbed by the underlying land surface is mainly determined by the land surface albedo, which plays an key role in the ground radiant energy balance [8], [17], [5]. Vegetation cover is an important parameter for evaluating the vegetation restoration conditions in degraded grasslands or farmland. Due to its sensitivity to the change condition of vegetation, NDVI has been widely used to analyze the land cover change and desertification process [18]–[20]. However, the vegetation condition cannot be well reflected in regions with sparse vegetation or higher vegetation coverage due to the influence of the soil background or saturation effect on the NDVI [8]. Therefore, the MSAVI, fully considering the bare soil line problem, has been introduced to deal with the effects of the vegetation canopy and soil background [8], [10]. The texture of topsoil has significant relationship to land degradation. Different levels of desertification lead to different surface topsoil textures. The desertification would be more severe while the topsoil grain composition becomes coarser. Coarsening of surface soil is a better indicator of land degradation, thus the grain size composition of topsoil can be utilized to reveal the process of land degradation [8], [18], [21], [22].

The reflectance data of six bands of Landsat8 OLI, including red, near infrared, blue, green, and short wave infrared band were utilized to inverse the above typical indices. The formulas for Albedo, NDVI, MSAVI, and TGSI were as follows [8]:

$$\begin{aligned} Albedo &= 0.356B_{\text{blue}} + 0.13B_{\text{red}} + 0.373B_{\text{nir}} \\ &\quad +0.085B_{\text{swir1}} + 0.072B_{\text{swir2}} - 0.0018 \quad (1) \\ \text{NDVI} &= (B_{\text{nir}} - B_{\text{red}})/(B_{\text{nir}} + B_{\text{red}}) \quad (2) \\ \text{MSAVI} &= (2B_{\text{nir}}+1-\sqrt{(2B_{\text{nir}}+1)^2-8(B_{\text{nir}}-B_{\text{red}})})/2 \quad (3) \\ \text{TGSI} &= (B_{\text{red}} - B_{\text{blue}})/(B_{\text{red}} + B_{\text{blue}} + B_{\text{green}}) \quad (4) \end{aligned}$$

where Bblue, Bgreen, Bred, Bnir, Bswir1, and Bswir2 referred to the reflectance of blue band, green band, red band, near-infrared band, shortwave infrared band 1 and 2, respectively.

C. STANDARDIZATION OF INDICES

In order to eliminate the differences in magnitude, the following Eq.(5) was utilized to standardize the data of different Indices [23].

$$I_{\text{nor},i} = \frac{I_i - I_{i,\text{CL}=0.05}}{I_{i,\text{CL}=0.95} - I_{i,\text{CL}=0.05}} \quad (5)$$

where Inor,i denoted the normalized indices i; Ii denoted the indices i; Ii,CL = 0.05 denoted the value of indices Ii where the confidential level(CL) was 0.05; I i,CL = 0.95 denoted the value of indices i where the confidential level(CL) was 0.95.

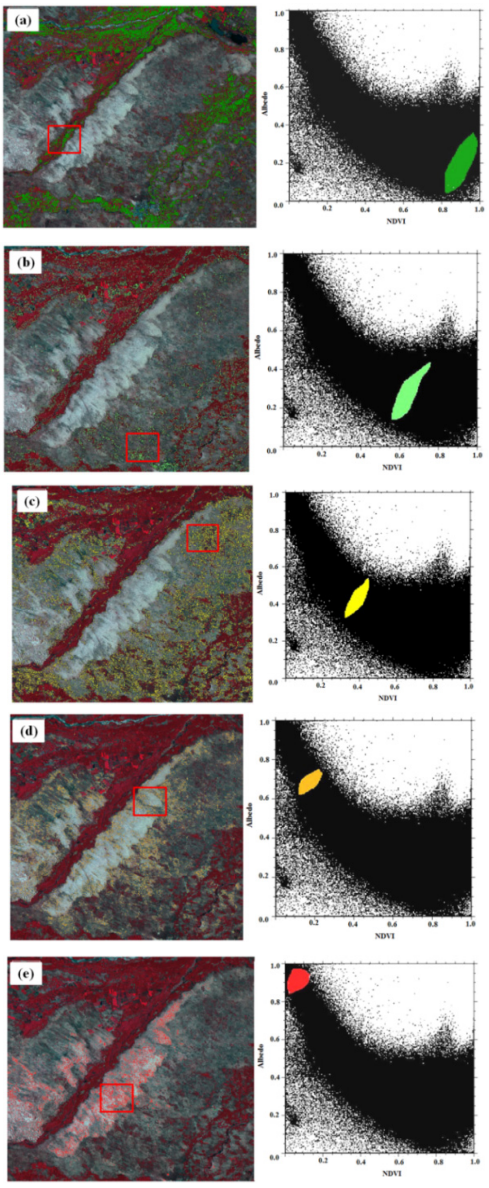

FIGURE 3. Different levels of desertification in image and Albedo-NDVI feature space. (a) Slight desertification; (b) mild desertification; (b) moderate desertification; (c) intensive desertification; (d) severe desertification.

III. EXPERIMENTAL RESULTS AND ANALYSIS

A. CONSTRUCTION OF THE FEATURE SPACE

As was shown in Figure 2, five feature spaces were constructed based on the above four sensitive indices, which were divided into two categories (first category: Albedo-MSAV; second category: Albedo-NDVI, Albedo-TGSI, TGSI-NDVI, and TGSI-MSAVI). In this paper the feature spaces of Albedo-NDVI and Albedo-MSAV were chosen to analyze the differences between the first category and second category.

B. ANALYSIA OF DESERTIFICATION PROCESS IN FEATURE SPACE

Figure 3 showed that there were significant differences in spatial distributions of different levels of desertification in

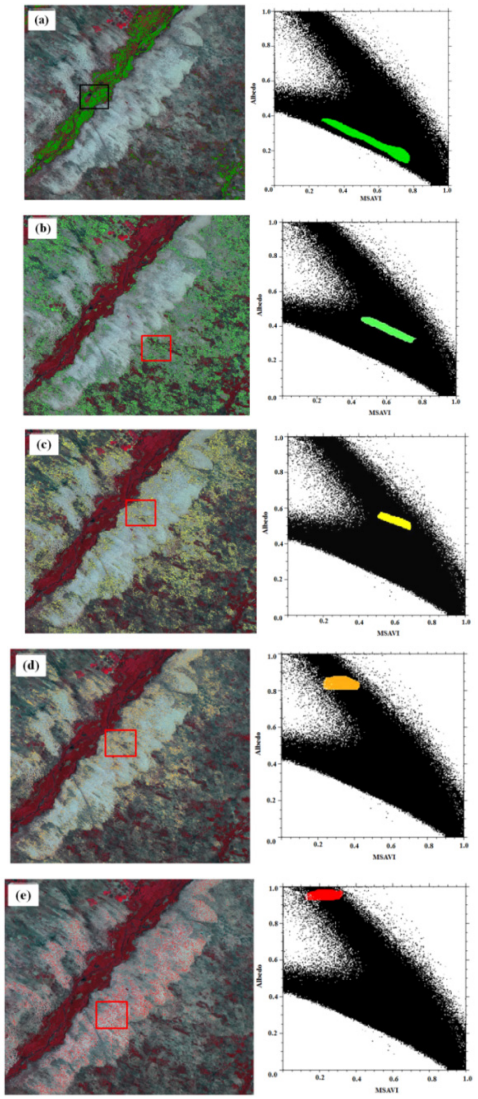

FIGURE 4. Different levels of desertification in image and Albedo-MSAVI feature space. (a) Slight desertification; (b) mild desertification; (c) moderate desertification; (d) intensive desertification; (e) severe desertification.

Albedo-NDVI feature space. The vegetation coverage would become lower with the increasing levels of the desertification. Five point clusters that distributed in different regions in the Albedo-MSAVI feature space were selected according to the distance to the point (1, 0). Then, the actual spatial distribution for each point cluster was analyzed to investigate the relationships among levels of desertification and five point clusters. Figure 3 showed that different levels of desertification (slight desertification, mild desertification, moderate desertification, intensive desertification and severe desertification) were concentrated in different regions in the Albedo-MSAVI feature space.

Similar to Figure 3, five point clusters have been selected according to the distance to soil line (Figure 4). Different levels of desertification were concentrated in different regions of the Albedo-MSAVI feature space. In addition, there was

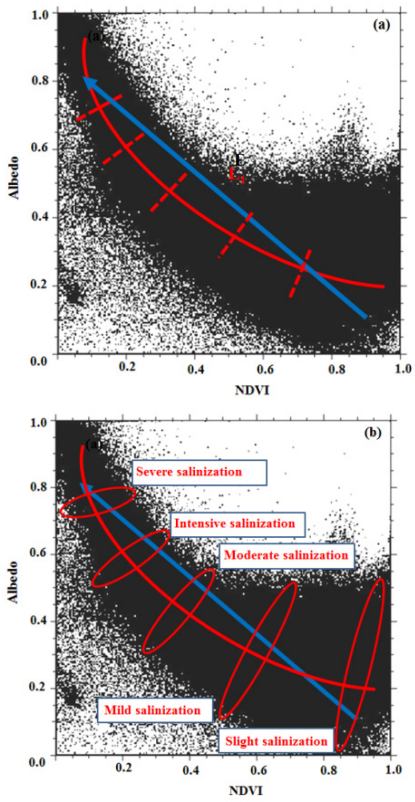

FIGURE 5. Albedo-NDVI feature space: (a) model of desertification index; (b) different levels of desertification in feature space.

significant relationship between different levels of desertification and point clusters.

C. MONITORING MODELS OF DESERTIFICATION

Figure 5 showed that the non-linear relationship between Albedo and NDVI was obvious, which could better indicate the process of desertification in the feature space. The straight line perpendicular to the red curve could distinguish different levels of desertification. Moreover, the spatial moving trajectory of the vertical direction in Albedo-NDVI feature space could be well fitted by a simple binary linear equation [24] (Eq. (6)):

$$\mathrm{DI} = \lambda \times \mathrm{NDVI} - \mathrm{Albedo} \tag{6}$$

where DI refers to the desertification index and λ was obtained based on the slope of the fitted straight line in the feature space.

Figure 6 showed that the desertification process could be explained by the distance from any point in the feature space to line L. The desertification would be more serious while the distance from line L became father. Based on the distance formula between point and line, the distance L2 from any point P in the Albedo-MSAVI feature space to line L could be expressed as follows [25]:

$$\mathrm{Albedo} = \alpha \mathrm{MSAVI} + \beta \tag{7}$$

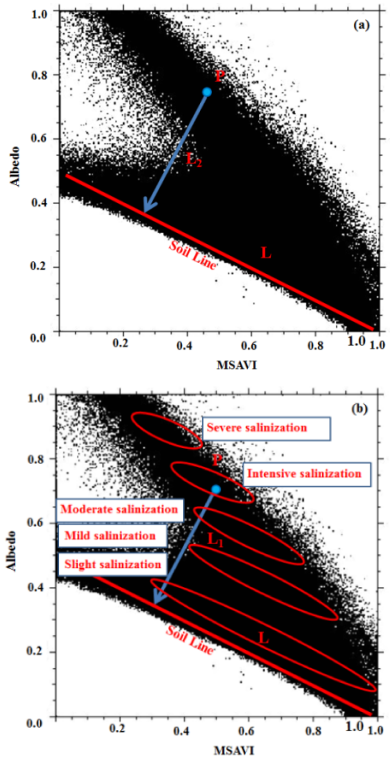

FIGURE 6. Albedo-MSAVI feature space: (a) model of desertification index; (b) different levels of desertification in feature space.

$$\mathrm{DI} = L_2 = \frac{|\mathrm{Albedo} - \alpha \mathrm{MSAVI} - \beta|}{\sqrt{1+\alpha^2}} \tag{8}$$

where DI was desertification index; λ and β were the parameters of the regression equation for soil line L in the feature space.

D. QUANTITATIVE RELATIONSHIPS AMONG FEATURE SPACE VARIABLES

The formula of soil line for Albedo-MSAVI feature space was shown in Figure 7(a), so the α and β for Equation 7 and 8 were −0.46 and 0.97, respectively. The linear formulas and correlation coefficient results of the other four feature space (Albedo-NDVI, Albedo-TGSI, TGSI-NDVI, and TGSI-MSAVI) were shown in Figure 7(b–e). There were significantly negative relationship between NDVI and Albedo, TGSI with the correlation indexes of 0.75 and 0.83, respectively. The correlation between TGSI and MSAVI, Albedo were positive with the correlation indexes of 0.68 and 0.30(weakly positive), respectively. Therefore, the feature space models of Albedo-MSAVI, Albedo-NDVI, Albedo-TGSI, and TGSI-NDVI were adopted to monitor the desertification information (Table 1).

IV. DISCUSSION

Utilizing the four feature space models, the desertification index of Naiman Banner have been calculated. Based on previous studies [8], [15], the desertification indexes of four feature space models were divided into five categories (Table2) to obtain the spatial distributions of different levels

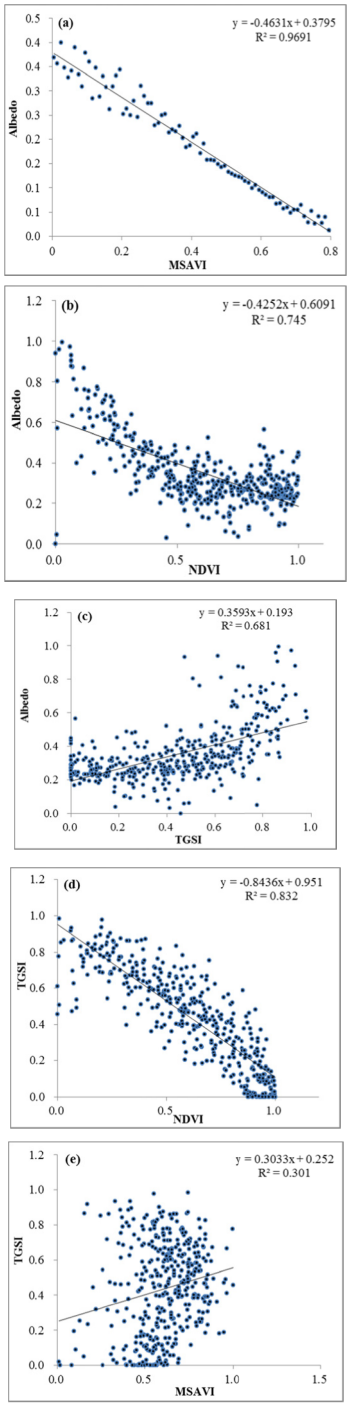

FIGURE 7. Correlation among variables of different feature spaces. (a) Albedo-MSAVI; (b) Albedo-NDVI; (c) Albedo-TGSI; (d) TGSI- NDVI; (e) TGSI-MSAVI.

of desertification (Figure 8) by Natural Breaks method of ArcGIS 10.2, which could better reflect the spatial difference among levels of desertification.

In order to test and verify the reversion precisions for different classifications of desertification, 210 sites from zones with different vegetation landscape patterns were selected with Google Earth and field observations (taking Albedo-MSAVI as an example, Table 3). The overall precision of

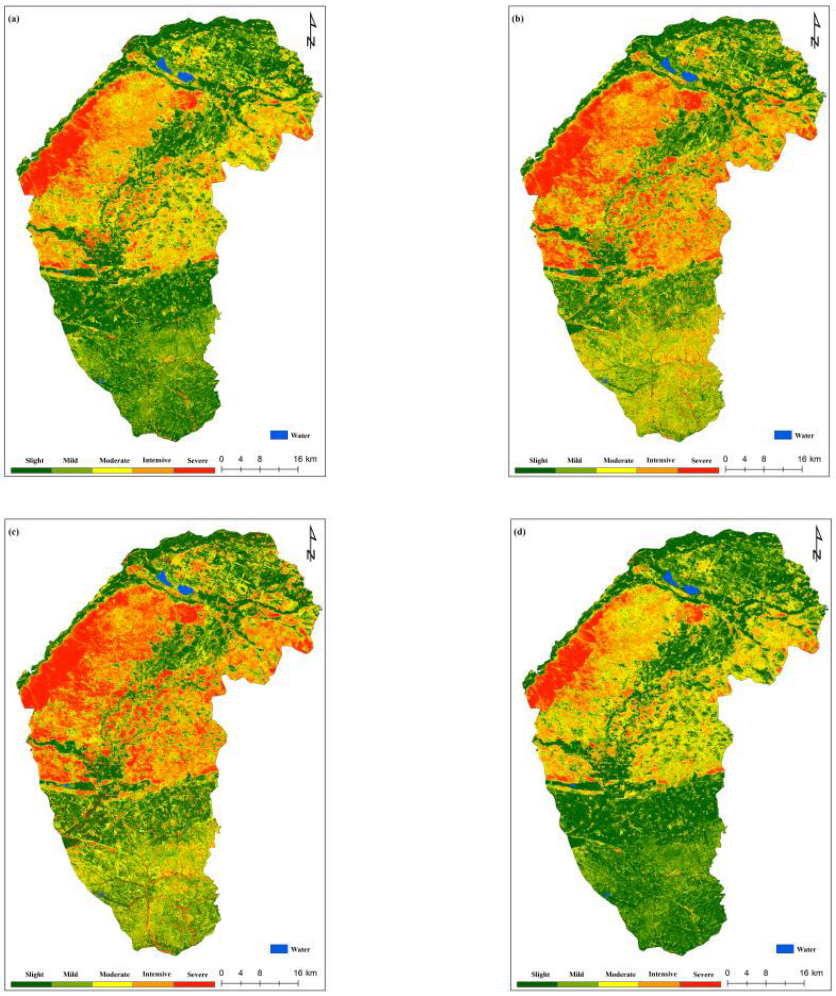

FIGURE 8. Spatial distributions of different levels of desertification. (a) Albedo-NDVI; (b) Albedo – TGSI; (c) TGSI-NDVI; (d) Albedo-MSAVI.

TABLE 1. Statistical parameters for the four feature space models.

Feature space models	λ	α	β
Albedo-NDVI	2.23	-	-
Albedo-TGSI	-2.78	-	-
TGSI-NDVI	1.19	-	-
Albedo-MSAVI	-	-0.46	0.38

TABLE 2. Classification thresholds of different levels of desertification.

Level	Albedo-MSAVI	Albedo-NDVI	Albedo-TGSI	TGSI-NDVI
Slight	<0.16	>1.50	>-0.8	>0.79
Mild	0.16-0.25	0.96-1.50	-1.50--0.8	0.36-0.79
Moderate	0.25-0.35	0.41-0.96	-2.12--1.5	-0.06-0.36
Intensive	0.35-0.48	-0.19-0.41	-2.73--2.12	-0.43--0.06
Severe	>0.48	<-0.19	<-2.73	<-0.43

four feature space models differed greatly (Figure 9). The feature space model of Albedo-MSAVI for Naiman Banner had the highest efficiency with the overall precision of 90.1%. The reason was that model of Albedo-MSAVI had fully considered the non-linear relationship between Albedo-MSAVI. Moreover, MSAVI, considering the bare soil line problem, had been introduced to eliminate the influence of the vegetation canopy and soil background [8], [19], [20]. The

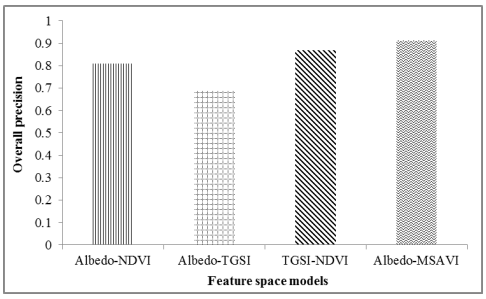

FIGURE 9. Overall precision comparisons of different feature space models.

TABLE 3. Error matrix of desertification categories(Albedo-MSAVI).

Error matrix		Inversed value					
		A	B	C	D	E	F
Observe d value	A	65	2	1	1	1	70
	B	0	45	0	1	0	46
	C	1	3	26	1	1	32
	D	0	1	2	25	1	29
	E	2	1	0	1	29	33
	F	68	52	29	29	32	210

Notes:A refers to Slight desertification;B refers to Mild desertification;C refers to Moderate desertification;D refers to Intensive desertification;E refers to Severe desertification;F refers to Sum.

overall precisions of Albedo-NDVI and TGSI-NDVI were 0.81 and 0.87, respectively. It was because that the vegetation condition could not be well reflected in NDVI for regions with sparse vegetation or higher vegetation coverage due to the interruption of bare land and reflectance saturation effect [10], [17], [23]. Thus, the inversion precision of regions with intensive and severe desertification was lower. The feature space model of Albedo-TGSI showed the worst precision with 0.69. This model had ignored the surface vegetation condition, which could greatly affect the process of land desertification [5], [14]. Overall, the feature space model of Albedo-MSAVI had high applicability for monitoring the desertification information in Naiman Banner.

V. CONCLUSION

Fully considering the influencing factors of the desertification process in Naiman Banner, four sensitive indices including MSAVI, NDVI, TGSI, and Albedo have been selected to construct five feature spaces. Then, precisions of different desertification monitoring models that derived from feature space (including non-linear and linear models) have been compared and analyzed. The non-linear Albedo-MSAVI feature space model for Naiman Banner has the highest efficiency with the overall precision of 90.1%, while the feature space model of Albedo-TGSI had the worst precision with 0.69. Overall, the feature space model of Albedo-MSAVI has the highest applicability for monitoring the desertification information in Naiman Banner.

REFERENCES

[1] C.-L. Zhang, Q. Li, Y.-P. Shen, N. Zhou, X.-S. Wang, J. Li, and W.-R. Jia, "Monitoring of aeolian desertification on the Qinghai–Tibet plateau from the 1970s to 2015 using landsat images," *Sci. Total Environ.*, vols. 619–620, pp. 1648–1659, Apr. 2018.

[2] J.-Y. Li, B. Xu, X.-C. Yang, Y.-X. Jin, Y.-Y. Li, J. Zhang, L.-N. Zhao, and R.-I. Li, "Dynamic changes and driving force of grassland sandy desertification in Xilin Gol: A case study of Zhenglan Banner," *Geograph. Res.*, vol. 30, no. 9, pp. 1669–1682, 2011.

[3] J. Yang, P. J. Weisberg, and N. A. Bristow, "Landsat remote sensing approaches for monitoring long-term tree cover dynamics in semi-arid woodlands: Comparison of vegetation indices and spectral mixture analysis," *Remote Sens. Environ.*, vol. 119, pp. 62–71, Apr. 2012.

[4] Q. Guo, B. Fu, P. Shi, T. Cudahy, J. Zhang, and H. Xu, "Satellite monitoring the spatial–temporal dynamics of desertification in response to climate change and human activities across the Ordos Plateau, China," *Remote Sens.*, vol. 9, no. 6, p. 525, May 2017.

[5] J. Li, X. Yang, Y. Jin, Z. Yang, W. Huang, L. Zhao, T. Gao, H. Yu, H. Ma, Z. Qin, and B. Xu, "Monitoring and analysis of grassland desertification dynamics using Landsat images in Ningxia, China," *Remote Sens. Environ.*, vol. 138, pp. 19–26, Nov. 2013.

[6] J. Rubio and E. Bochet, "Desertification indicators as diagnosis criteria for desertification risk assessment in Europe," *J. Arid Environ.*, vol. 39, no. 2, pp. 113–120, Jun. 1998.

[7] G. Hu, Z. Dong, J. Lu, and C. Yan, "The developmental trend and influencing factors of Aeolian desertification in the Zoige Basin, Eastern Qinghai–Tibet Plateau," *Aeolian Res.*, vol. 19, pp. 275–281, Dec. 2015, doi: 10.1016/j.aeolia.2015.02.002.

[8] H. Wei, J. Wang, K. Cheng, G. Li, A. Ochir, D. Davaasuren, and S. Chonokhuu, "Desertification information extraction based on feature space combinations on the mongolian plateau," *Remote Sens.*, vol. 10, no. 10, p. 1614, Oct. 2018.

[9] M. M. Boer and J. Puigdefábregas, "Assessment of dryland condition using spatial anomalies of vegetation index values," *Int. J. Remote Sens.*, vol. 26, no. 18, pp. 4045–4065, Sep. 2005.

[10] Y. Zeng, Z. Feng, and N. Xiang, "Albedo-NDVI space and remote sensing synthesis index models for desertification monitoring," *Scientia Geographica Sina* vol. 26, no. 1, pp. 75–81, 2006.

[11] M. Dawelbait and F. Morari, "Monitoring desertification in a Savannah region in Sudan using Landsat images and spectral mixture analysis," *J. Arid Environ.*, vol. 80, pp. 45–55, May 2012.

[12] N. Zhang, X. L. Chang, X. Y. Sun, and Y. Han, "Ecological security assessment of Naiman County based on desertification degree and NDVI index," *Chin. J. Ecol.*, vol. 29, no. 6, pp. 1250–1256, 2010.

[13] X. D. Ge and Z. S. Li, "Distribution of sandy desertification around surface waters in Horqin Sandy land: Case study in Naiman banner," *J. Desert Res.*, vol. 29, no. 3, pp. 404–408, 2009.

[14] Z. Ma, Y. Xie, J. Jiao, L. Li, and X. Wang, "The construction and application of an Aledo–NDVI based desertification monitoring model," *Procedia Environ. Sci.*, vol. 10, pp. 2029–2035, Sep. 2011.

[15] Y. Q. Ren, H. L. Liu, L. X. Tang, L. L. Jiang, and X. Y. An, "A study on dynamic changes of desertification in south edge of Junggar basin based on NDVI-albedo features," *Bull. Soil Water Conservation*, vol. 34, no. 2, pp. 267–271, 2014.

[16] Z. Wu, S. Lei, Z. Bian, J. Huang, and Y. Zhang, "Study of the desertification index based on the albedo-MSAVI feature space for semi-arid steppe region," *Environ. Earth Sci.*, vol. 78, no. 6, Mar. 2019.

[17] Y. Zeng and Z. Feng, "Advances in sandy desertification detecting and its environmental impacts," (in Chinese), *J. Mountain Sci.*, vol. 23, no. 2, pp. 218–227, Mar. 2005.
[18] M. Lamchin, J.-Y. Lee, W.-K. Lee, E. J. Lee, M. Kim, C.-H. Lim, H.-A. Choi, and S.-R. Kim, "Assessment of land cover change and desertification using remote sensing technology in a local region of Mongolia," *Adv. Space Res.*, vol. 57, no. 1, pp. 64–77, Jan. 2016.
[19] H.-L. Zhao, J. Li, R.-T. Liu, R.-L. Zhou, H. Qu, and C.-C. Pan, "Effects of desertification on temporal and spatial distribution of soil macro-arthropods in Horqin sandy grassland, Inner Mongolia," *Geoderma*, vols. 223–225, pp. 62–67, Jul. 2014.
[20] J. Qi, A. Chehbouni, A. Huete, Y. Kerr, and S. Sorooshian, "A modified soil adjusted vegetation index," *Remote Sens. Environ.*, vol. 48, no. 2, pp. 119–126, May 1994.
[21] C. Zucca, R. D. Peruta, R. Salvia, S. Sommer, and M. Cherlet, "Towards a world desertification Atlas. Relating and selecting indicators and data sets to represent complex issues," *Ecol. Indicator*, vol. 15, pp. 157–170, Apr. 2012.
[22] Q. Li, C. Zhang, Y. Shen, W. Jia, and J. Li, "Quantitative assessment of the relative roles of climate change and human activities in desertification processes on the Qinghai–Tibet Plateau based on net primary productivity," *Catena*, vol. 147, pp. 789–796, Dec. 2016.
[23] B. Guo, F. Yang, B. Han, Y. Fan, S. Chen, W. Yang, and L. Jiang, "A model for the rapid monitoring of soil salinization in the yellow river delta using landsat 8 OLI imagery based on VI–SI feature space," *Remote Sens. Lett.*, vol. 10, no. 8, pp. 796–805, Aug. 2019.
[24] M. Verstraete and B. Pinty, "Designing optimal spectral indexes for remote sensing applications," *IEEE Trans. Geosci. Remote Sens.*, vol. 34, no. 5, pp. 1254–1265, Sep. 1996.
[25] B. Guo, F. Yang, Y. Fan, B. Han, S. Chen, and W. Yang, "Dynamic monitoring of soil salinization in yellow river delta utilizing MSAVI–SI feature space models with Landsat images," *Environ Earth Sci.*, vol. 78, no. 10, p. 308, May 2019.

BING GUO was born in Zibo, Shandong, in 1987. He received the B.S. degree in geographic information system from Ludong University, Yantai, in 2010, and the M.S. and Ph.D. degrees in cartography and geographical information system from the University of Chinese Academy of Sciences, Beijing, in 2013 and 2016, respectively.

From 2016 to 2019, he was a Lecturer with the School of Civil Architectural Engineering, Shandong University of Technology. He is the author of one book and more than 50 articles. His research interests include remote sensing, ecological environment, natural hazards, global change, and land use change.

Dr. Guo was a member of the Member of Chinese Geographical Society. He was a recipient of the Dean Excellence Award of University of Chinese Academy of Sciences and the Excellent Thesis Award of Journal of Arid land, in 2018.

YE WEN was born in Heilongjiang, in 1987. She received the B.S. degree in geographic information system from the Heilongjiang Institute of Technology, Harbin, in 2010, and the M.S. degree in geodesy and survey engineering from Liaoning Technical University, Fuxin, in 2013. She is currently pursuing the Ph.D. degree in land use and information technology with Shenyang Agricultural University.

From 2013 to 2019, she was a Lecturer with the School of Architectural Engineering, City Institute, Dalian University of Technology. Her research interests include remote sensing, soil information, land use change, and ecological environment.